Hydrocarbon reservoir thickness resolution in 3D CSEM anisotropic inversion

Jan Petter Morten, Astrid Kornberg Bjørke, and Anh Kiet Nguyen, EMGS

Summary

We describe a regularization approach to enhance hydrocarbon reservoir thickness imaging in anisotropic 3D inversion of controlled source electromagnetic (CSEM) data, utilizing measurements in the broadside source-receiver in complement with in-line configuration measurements. In order to capture the thickness information from the broadside measurements, model constraints are needed in anisotropic inversion to couple the vertical and horizontal resistivity components. The proposed regularization approach provides *a priori* constraints on the anisotropy factor. We present 3D inversion results that show how the regularization avoids unrealistic representation of a thin, isotropic reservoir response by a thick and strongly anisotropic resistor.

Introduction

CSEM surveying for hydrocarbon reservoirs in 3D rather than 2D line geometry has proved to significantly expand the applicability of the method. In a 3D survey, data is recorded by receivers both on and off the horizontal electric dipole source towline. Benefits of 3D acquisition include detection of smaller targets in coarse receiver grids (Morten *et al*., 2009), lateral delineation and volume estimates for appraisal (Gabrielsen *et al*., 2009), and increased target confidence through improved understanding of background resistivity trends and anisotropy (Jing *et al*., 2008).

The utility of the data is improved by advanced processing schemes like inversion, which make use of all information in the dataset and not only anomalies related directly to interaction with the reservoir. Increased level of detail in reservoir imaging is possible in 3D inversion by incorporating measurements that are only sensitive to thick reservoirs. In areas with limited structural information about reservoirs, it can be difficult to formulate inversion constraints so it becomes especially important to make use of all information about the reservoir contained in the CSEM data.

Two qualitatively different types of measurements will be captured in a 3D survey: Data recorded in-line with the symmetry axis of the horizontal electric dipole source, and data recorded transversal to this axis (broadside data). Data recorded at other positions with intermediate azimuth can be described as a superposition of these types (Maaø *et al*., 2007). Note that in-line measurements using a source with dipole components transversal to the towline also provides broadside data.

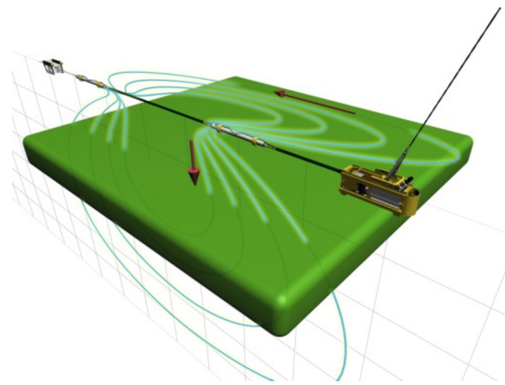

Figure 1: Source dipole field lines illustrated on resistor. In-line measurement geometry (along dipole) generates electric field lines penetrating resistor with a dominant vertical component, whereas broadside measurement geometry (transverse to dipole) mainly generates electric field interacting horizontally with resistor.

As observed in isotropic 1D modeling and inversion by Constable and Weiss (2006), and also discussed by Key (2009), reservoir thickness reconstruction is enhanced by broadside data in complement to in-line data.

Qualitatively, we may describe reservoir responses detected in the in-line configuration as a result of series coupling of the conductive background and the resistive reservoir. This heuristic is illustrated in Figure 1, where electric field lines in the vertical plane of the source towline interact with the resistor with a large vertical vector component. An electrical current is thus driven in series with the horizontal reservoir, and gives a response measured as in-line data. The effective resistivity will be dominated by the reservoir. This is the effect utilized in CSEM hydrocarbon exploration (Constable and Srnka, 2007).

Measurements in the broadside configuration, on the other hand, can be described as resulting from a parallel coupling of the reservoir and the formation. The electric field lines in Figure 1 extending out of plane indicate a predominantly horizontal electric field interacting with the resistor. In this configuration, a thin resistive layer gives a very small modification of the background response, since the resistor covers a small vertical cross-section of the area probed by the electric field. The response scales with the thickness of the reservoir, so that reservoirs with thickness comparable to the smallest length scales of the measurement give significant anomalous responses also in the broadside configuration. For a typical low-frequency CSEM measurement this length scale is given by the skin-depth, which can vary from a few hundred meters to the kilometer scale.

© 2010 SEG

In this paper, we analyze the in-line and broadside responses from a synthetic 3D model, varying the resistor thickness. This setup demonstrates quantitatively the different type of information available from in-line and broadside measurements, and indicates that reservoir geometry reconstruction should benefit from broadside data, in agreement with Constable and Weiss (2006). Anisotropic environments pose a complication for full utilization of the reservoir thickness information in the broadside data. Representing the subsurface as a transverse isotropic model with a vertical axis of symmetry (TIV), separate vertical and horizontal components of the resistivity tensor are used. The in-line and broadside responses will then to a large degree couple independently to the vertical and horizontal components, respectively. Specifically, the response from an isotropic thin resistive layer may be represented by a thick resistor in only the vertical resistivity component. We address this problem by introducing a regularization approach to couple the two resistivity components. The improvement in resistor reconstruction is demonstrated by 3D inversion results.

In-line and broadside data responses

The synthetic 3D model studied has a disc shaped resistor of diameter 6 km embedded in a homogeneous background. The background resistivity is 2 and $\frac{2}{3}$ Ωm for the vertical and horizontal components. The water depth is 1 km, and the center of the resistor is 2 km depth below the seafloor. We vary the resistor thickness, and keep resistivity times thickness constant at 4000 Ωm^2. The so-called T-equivalence (Constable and Weiss, 2006) denotes that equivalent CSEM responses may be obtained from different resistors with the same resistivity-thickness product. The validity of this approximate relationship can be studied in the data shown in Figure 2. In the top row, we show the in-line responses of a thick (500 m, 8 Ωm) and a thin (50 m, 80 Ωm) resistor. The receiver and towline configurations are indicated by thick lines in Figure 3. Comparing the right and the left panel one can see that the normalized in-line responses indeed differ little: 0.05 to 0.10 at a given frequency and offset. However, the non-monotonous frequency variances discern different geometries.

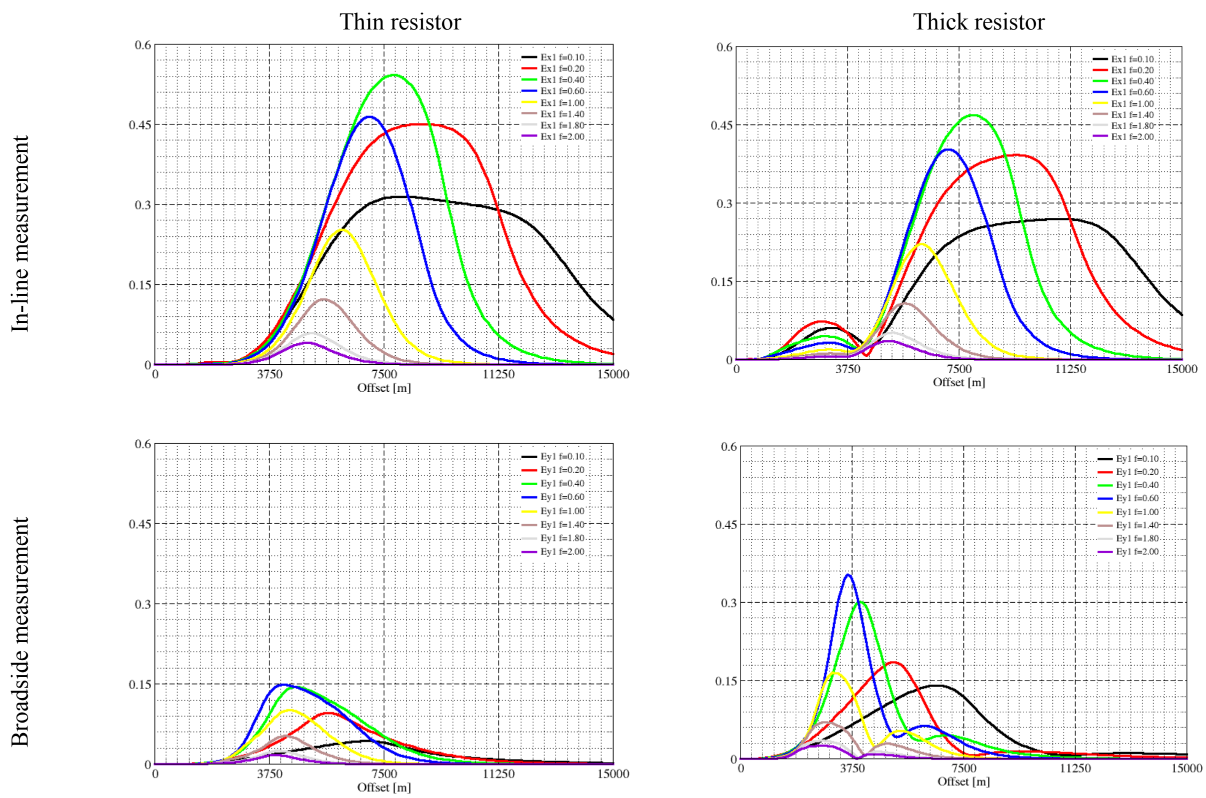

Figure 2: Synthetic responses for thin (50 m, left) and thick resistors (500 m, right) for in-line measurement geometry (top) and broadside measurement geometry (bottom). The reservoir response is computed as $|E_{\text{Resistor}} - E_{\text{Background}}|/(|E_{\text{Background}}| + \delta)$ where E is the complex electric field, and δ is a typical noise level 10^{-15} V/m.

© 2010 SEG

Broadside data computed for the same models is shown in the lower row of Figure 2. The source dipole and the electric field measurement were transverse to the towline heading. In contrast to the similarity of the in-line responses, the broadside data for the thin and the thick resistors differ substantially. While the difference in in-line responses of the thin and the thick resistors was less than 20 %, the difference in broadside data response is up to 130 %. For the thin resistor, the normalized response in the broadside configuration is below 0.15, which in a complex geological environment would be challenging to identify from the background response (Hesthammer, 2010). The broadside response of the thick resistor, on the other hand, can be as high as 0.35 which is a strong response feasible for detection even by anomaly mapping. This example thus clearly demonstrates that significant information about the geometry of resistive targets may be obtained from broadside data, with immediate potential for improved reservoir understanding through 3D inversion.

Thin resistor imaging in anisotropic environments

The small response from the thin reservoir in broadside data that we studied above, is due to the horizontal direction of the generated electric field. An implication of these results is that the broadside data is more sensitive to the horizontal than the vertical component of the resistivity. Conversely, the in-line data is more sensitive to the vertical resistivity component. This has important consequences for anisotropic inversion of responses from thin resistors. The in-line data responses require a resistor reconstruction in the vertical resistivity component, but as demonstrated above the response is non-unique and can be represented as a thin or a thick resistor. A thick resistor complies more with the inherent, long length scales of the CSEM measurement. Since the broadside response from the thin resistor is very small, the reconstruction into the horizontal resistivity component can be very weak. This will result in large anisotropy even though the true resistor is isotropic. In summary, a thin isotropic resistor response will typically be inverted as a thick anisotropic resistor with the same resistivity-thickness product in the vertical resistivity component only.

The incorrect results that can arise from anisotropic inversion of thin resistor responses is due to the non-uniqueness of in-line responses, and also the decoupling of sensitivity to vertical and horizontal resistivity components in in-line and broadside data. Whereas the former is an intrinsic aspect of the measurement, the latter can be viewed as a weakness of the model representation and imaging procedure. We propose to introduce a coupling of the two resistivity components by providing *a priori* information about the maximum expected anisotropy factor

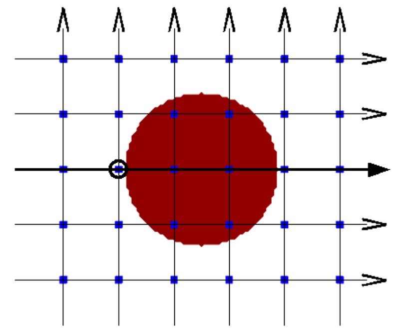

Figure 3: Receiver layout and location of resistor in true model. The receiver spacing is 2 km. Source towlines over all *x*- and *y*-directed receiver lines are included in the complete dataset.

of the subsurface. This approach will limit the model space that explain the data, so that inverted models with volumes of high resistivity in the vertical component and unrealistically strong anisotropy are avoided. Rather, a resistor must be introduced both in the vertical and horizontal resistivity components in order not to exceed the *a priori* bound on the anisotropy. In this way, the absence of a response from thin resistors in broadside data acts as a geometrical constraint on the reconstruction. The non-unique in-line response may be represented only as a thin resistor, since a thick resistor reconstruction would be incompatible with the absence of a broadside data response.

3D inversion with *a priori* anisotropy regularization

The software used to create inverted 3D models in this paper has been described by Zach *et al.* (2008). We have implemented the following regularization functional to introduce *a priori* information about the anisotropy factor $R=\rho_V/\rho_H$.

$$\varepsilon_{ap} = \sum_{i,j,k} \frac{W_{i,j,k}}{N_{cells}} \left[\Theta\left(R^{lower}_{i,j,k} - R_{i,j,k}\right)\left(R^{lower}_{i,j,k} - R_{i,j,k}\right)^2 + \Theta\left(R_{i,j,k} - R^{upper}_{i,j,k}\right)\left(R_{i,j,k} - R^{upper}_{i,j,k}\right)^2 \right].$$

Here i,j,k are indices for the cells of the 3D model grid, $W_{i,j,k}$ is a weight grid, N_{cells} is the number of cells to be updated by the inversion, and Θ is the Heaviside step function. The regularization cost of surpassing the upper (R^{upper}) or lower (R^{lower}) *a priori* anisotropy factor scales quadratically with the deviation at each cell. Whenever the anisotropy factor is between the upper and lower bounds, the regularization vanishes. In areas where little information about the anisotropy is available, inversion without this regularization should be carried out first to get an estimate of the typical anisotropy factor of the background. If other measurements of the electrical resistivity anisotropy are available *e.g.* from deviated or tri-

© 2010 SEG

axial well logs, such information can be used to construct the bounds. Moreover, structural information or varying degree of certainty of the expected anisotropy can be taken into account since both the weight and the bounds can be spatially dependent. For example, if the location of an isotropic sandstone reservoir in an anisotropic formation is known from seismic, a lower bound on the upper anisotropy factor can be applied in the reservoir zone than elsewhere in the formation.

We have carried out 3D inversion of the synthetic data for the thin resistor model studied above with an isotropic 50 m thick resistor, using data from all receivers indicated in Figure 3. Data for horizontal components of the electric field at frequencies 0.2, 0.4, and 0.6 Hz were included in the inversion. Only data from those offset intervals where the electric field magnitude was above the typical noise floor (10^{-15} V/m) of real surveys was taken into account. A minimum gradient support regularization was applied (Zhdanov, 2002). The inversion results in the following have similar data fit for the offset ranges considered.

Sections from the final inverted 3D volumes along the towline highlighted in Figure 3 are shown in Figure 4. We show both the vertical and horizontal resistivity models, and results obtained without regularization and by using the *a priori* anisotropy regularization approach described above. We used R_{upper} = 3 and R_{lower} = 1 for the entire model. The initial model was the true background model. The results obtained without *a priori* anisotropy regularization show a thick (~500 m) resistor in the vertical resistivity model alone, as expected from the discussion above. Applying the *a priori* anisotropy regularization results in a much better approximation of the true model: a thinner resistor (~250 m) reconstructed into both resistivity components with a moderate anisotropy (close to the specified R_{upper}). The resistivity-thickness products calculated at the center of the resistor are interestingly closest to the true model for the case when the *a priori* anisotropy regularization was applied, although in both cases there is incorrect lateral variation.

Conclusions

We have demonstrated that information about the thickness of resistive bodies is contained in broadside CSEM data. In 3D CSEM this data gives enhanced resolution through isotropic inversion. In TIV anisotropic inversion, the additional degree of freedom typically leads to a degradation of thickness resolution and models where the resistor is present only in the vertical resistivity model, introducing an unrealistically high anisotropy. A proposed regularization approach to couple the two resistivity components reinstates the resistor thickness definition using a priori information about the anisotropy factor. This approach gives good results for the synthetic dataset studied in this paper, and has also been applied successfully for 3D inversion of real data from various geological settings. A challenge for the proposed regularization is reservoirs with strong anisotropy. In this case, structural information from seismic can be incorporated to provide constraints that enhance reservoir definition.

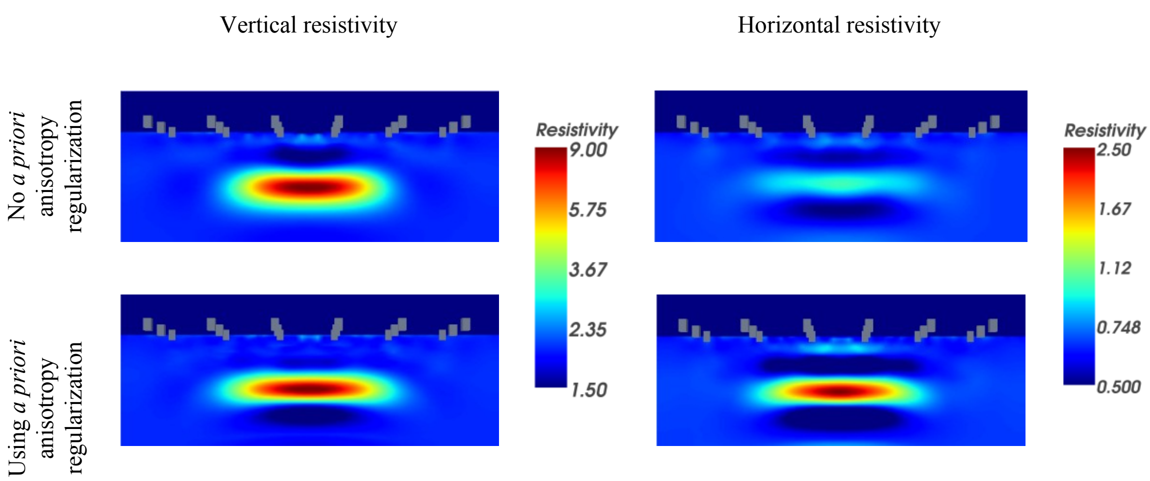

Figure 4: Vertical sections through center of final 3D inverted models for the thin (50 m) resistor model. The separate color scales for the vertical and horizontal resistivity are shown to the right of the plots.

© 2010 SEG

EDITED REFERENCES

Note: This reference list is a copy-edited version of the reference list submitted by the author. Reference lists for the 2010 SEG Technical Program Expanded Abstracts have been copy edited so that references provided with the online metadata for each paper will achieve a high degree of linking to cited sources that appear on the Web.

REFERENCES

Constable, S., and C. J. Weiss, 2006, Mapping thin resistors and hydrocarbons with marine EM methods: Insights from 1D modeling: Geophysics, **71**, no. 2, G43–G51.

Constable, S., and L. J. Srnka, 2007, An introduction to marine controlled-source electromagnetic methods for hydrocarbon exploration: Geophysics, **72**, no. 2, WA3–WA12.

Gabrielsen, P. T., I. Brevik, R. Mittet, L.O. Løseth, Investigating the exploration potential for 3D CSEM using a calibration survey over the Troll Field: First Break, **27**, no. 6.

Hesthammer, J., A. Stefatos, M. Boulaenko, S. Fanavoll, and J. Danielsen, 2010, CSEM performance in light of well results: The Leading Edge, **29**, 34, doi:10.1190/1.3284051.

Jing, C., K. Green, and D. Willen, 2008, CSEM inversion: Impact of anisotropy, data coverage, and initial models: 78th Annual International Meeting, SEG, Expanded Abstracts, 604–608.

Key, K., 2009, 1D inversion of multicomponent, multifrequency marine CSEM data: Methodology and synthetic studies for resolving thin resistive layers: Geophysics, **74**, no. 2, F9, doi:10.1190/1.3058434.

Maaø, F. A., 2007, Svein Erling Johnstad, Pål T. Gabrielsen, and Martin Panzner, Azimuth decomposition of SBL data: SEG Expanded Abstracts, **26**, 564.

Morten, J. P., A. K. Bjørke, T. Støren, E. Coward, S. A. Karlsen, and F. Roth, 2009, Importance of azimuth data for 3D inversion of marine CSEM scanning data: 71st Annual Conference and Exhibition, EAGE, Extended Abstracts.

Zach, J. J., A. K. Bjørke, T. Støren, and F. Maaø, 2008, 3D inversion of marine CSEM data using a fast finite-difference time-domain forward code and approximate hessian-based optimization: SEG Technical Program Expanded Abstracts, **27**, 614. doi:10.1190/1.3063726

Zhdanov, M. S., 2002, Geophysical inverse theory and regularization problems: Elsevier.

© 2010 SEG